Characterization of Oxidation Products from HOCl Uptake by Microhydrated Methionine Anions using Cryogenic Ion Vibrational Spectroscopy

Santino J. Stropoli,[a] Kim Greis,[a,b] Tim Schleif,[a] and Mark A. Johnson*[a]

[a] Sterling Chemistry Laboratory, Department of Chemistry, Yale University, New Haven, CT 06520, United States

[b] Institut für Chemie und Biochemie, Freie Universität Berlin, Altensteinstraße 23A, 14195 Berlin, Germany; Fritz-Haber-Institut der Max-Planck-Gesellschaft, Faradayweg 4–6, 14195 Berlin, Germany

* Email: mark.johnson@yale.edu

ABSTRACT:

The oxidation of the amino acid methionine (Met) by hypochlorous acid (HOCl) to yield methionine sulfoxide (MetO) has been implicated in both the interfacial chemistry of tropospheric sea spray aerosols as well as the destruction of pathogens in the immune system. Here, we investigate the reaction of deprotonated methionine water clusters $Met^-\cdot(H_2O)_n$ with HOCl and characterize the resulting products using cryogenic ion vibrational spectroscopy and electronic structure calculations. Capture of the $MetO^-$ oxidation product in the gas phase requires the presence of water molecules attached to the reactant anion. Analysis of its vibrational band pattern indicates that the sulfide group of Met^- has indeed been oxidized. The vibrational spectrum of the anion corresponding to uptake of HOCl by $Met^-\cdot(H_2O)_n$ indicates that it exists as an "exit-channel" complex, in which the Cl^- product ion is bound to the COOH group following formation of the S=O motif.

TOC GRAPHIC:

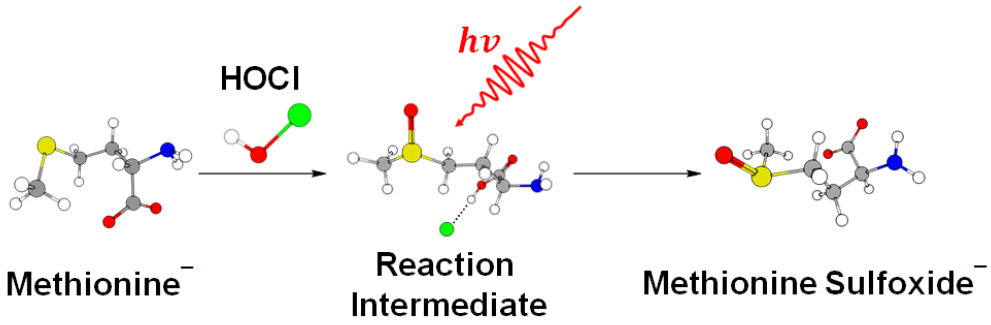

1. INTRODUCTION

The chemistry of hypochlorous acid (HOCl) has significant implications in both atmospheric[1-3] and biological chemistry.[4-5] In the troposphere, HOCl is thought to liberate dihalogens by interfacial reactions with halide-containing sea spray aerosol (SSA) particles as part of an autocatalytic, ozone-depleting cycle.[6-9] While this reaction is often cited as a key step in tropospheric halogen cycling,[1-3] little is known about the possible competing reactive pathways of HOCl, which may be relevant considering its high redox potential (+1.63 V)[10] and given that SSA can exhibit surprisingly large (> 0.8) organic mass fractions.[11-12] For example, the concentrations of amino acids (many of which are known to react with HOCl in the aqueous phase)[13] can be enhanced in SSA by up to 7 orders of magnitude relative to bulk seawater.[14] The oxidation of methionine (Met) by HOCl at its sulfur group to form methionine sulfoxide (MetO) is particularly fast ($k_2 \sim 10^7$ $M^{-1}s^{-1}$),[15] and recent studies have indicated that Met and other hydrophobic amino acids are driven to the surface of SSA.[16-17] In fact, preliminary work has suggested that addition of Met to laboratory-generated aerosols may dramatically increase the reactive uptake coefficient of HOCl.[18]

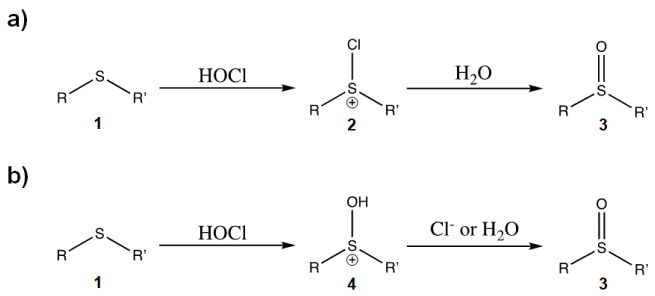

Scheme 1. Proposed mechanisms of sulfide oxidation by HOCl via (a) a chlorosulfonium intermediate or (b) an oxysulfonium intermediate.

While HOCl is known to react with a number of biological species,[4-5, 13, 19-22] sulfur-containing sidechains like that of Met are particularly susceptible targets given their rapid kinetics.[15, 23-24] There is, however, no clear consensus of the molecular-level mechanisms that drive these reactions. For example, one commonly invoked mechanism involves Met oxidation through a so-called "chlorine-transfer" to the sulfur atom, forming a short-lived "chlorosulfonium" intermediate (**2**) before being quickly hydrolyzed (**Scheme 1a**). Such chlorosulfonium-containing salts can be isolated from aprotic solutions,[25] but the chlorosulfonium ion intermediate in an oxidation reaction has never been directly observed in the aqueous phase.[15, 26-27] To address this issue, Ruff *et al*. explored the oxidation of sulfides by hypochlorites with DFT calculations and found that the barrier for chlorosulfonium formation is very high in the absence of solvent.[27] This led the authors to propose a more energetically favorable pathway which proceeds via direct attack by the oxygen atom of HOCl to form an oxysulfonium (**4**) species (**Scheme 1b**). This species may then yield the sulfoxide product through deprotonation by either Cl^- or H_2O. In a more recent follow up study, Ruff *et al*. predicted that the barriers for the pathways in **Schemes 1a** and **1b** become comparable as the number of solvent water molecules increases, as water may aid the departure of the poorer OH^- leaving group of HOCl.[28] Here we investigate the reaction of the isolated Met anion (Met^-) and its small clusters with water molecules [$Met^-\cdot(H_2O)_{n=0-8}$] with HOCl using a combination of gas-phase ion chemistry and spectroscopy methods. These experimental results are analyzed in the context of expectations based on the energetics and structures of stationary points on the potential energy surface obtained with electronic structure calculations. Specifically, the identities of product ions created by reactive HOCl uptake are determined by analysis of their vibrational spectra, which are measured using cryogenic ion vibrational spectroscopy.[29-31]

2. EXPERIMENTAL AND COMPUTATIONAL DETAILS

2.1. Experimental Setup

The reaction of Met with HOCl was investigated by collisions of $Met^-\cdot(H_2O)_n$ cluster ions with HOCl vapor in a radiofrequency (quadrupole) ion guide using the Yale cryogenic photofragmentation mass spectrometer.[32] A schematic diagram of the experimental arrangement is presented in **Figure 1**. Briefly, $Met^-\cdot(H_2O)_n$ cluster ions were generated by electrospray ionization (ESI) of a 4 mM solution of Met (L-methionine, Sigma-Aldrich, 98%) in 1:9 H_2O/CH_3CN in a humidity-controlled purge capsule at atmospheric pressure (i.e., CO_2-free air saturated with water vapor from a reservoir in the purge capsule). The ions then passed through an 0.635 mm × 5.6 cm long stainless-steel capillary followed by a 0.635 mm conical skimmer into the quadrupole collision cell. The collision cell was filled with room-temperature HOCl vapor introduced through a leak valve at a total chamber pressure of ~10^{-2} Torr. The HOCl sample was prepared using a phosphate-buffered solution of sodium hypochlorite as has been previously reported in detail.[33] Following reaction in the ~300 K ion guide, product ions were trapped and cooled to 77 K with pulsed helium buffer gas in a liquid nitrogen (LN_2)-cooled radio frequency (RF) octupole ion trap.[34] Ion packets were then extracted and guided into a cryogenic (~20 K) 3D Paul trap, where they were further cooled and "tagged" with H_2 using a mixture of 20% hydrogen and 80% helium before extraction into a triple-focusing time-of-flight photofragmentation mass spectrometer. Cold vibrational spectra of each species were then acquired by monitoring the photoevaporation of these weakly-bound H_2 tags in a linear action regime

$$M^- \cdot H_2 + h\nu \rightarrow M^- + H_2 \qquad (1)$$

as previously described.[29-31]

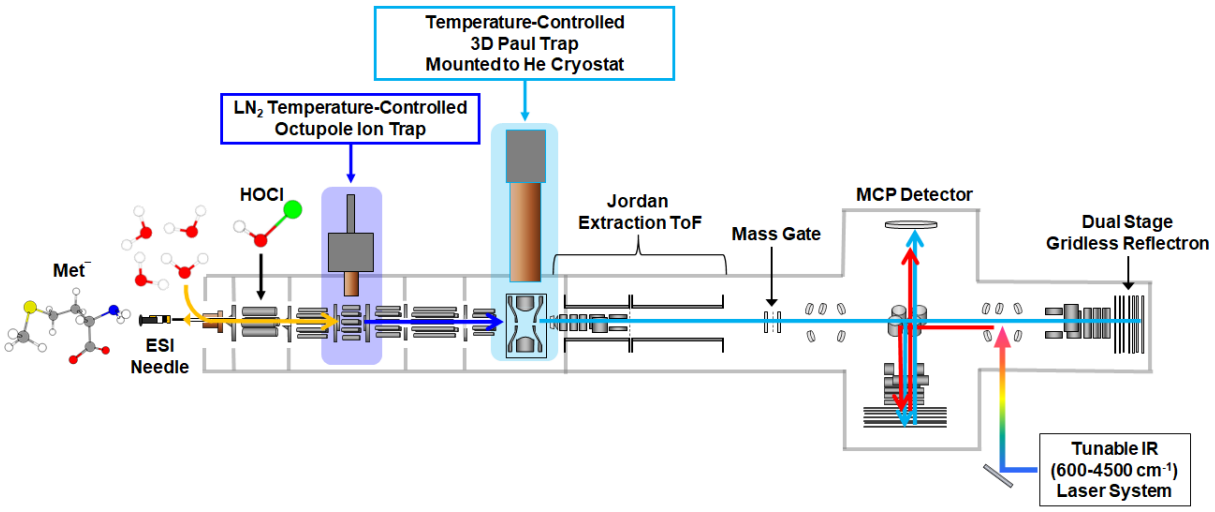

Figure 1. Schematic of the Yale instrument used in this study. $Met^-\cdot(H_2O)_n$ reactant clusters are generated by electrospray ionization in a humidity-controlled purge capsule before colliding with gaseous HOCl (~10^{-2} Torr) in the first quadrupole guide. The resulting products are collected in a 77 K octupole trap to form an ion packet that is transferred to a cryogenic (~20 K) 3D Paul Trap and tagged with H_2. Vibrational spectra are then acquired by infrared photodissociation of the weakly-bound H_2 tag.

2.2. Computational Details

The conformational spaces of deprotonated methionine, its HOCl adducts, and methionine sulfoxide [both (*R*,*S*) and (*S,S*)- epimers], as well as the $n = 1$ H_2O hydrates of deprotonated methionine and methionine sulfoxide were sampled using the CREST[35] tool with the semiempirical GFN2-xTB[36] method. The 20 lowest-energy conformers found using this method were reoptimized in Gaussian 16[37] at the PBE0+D3/6-31G(d)[38-40] level of theory. A subset of low-energy structures from this calculation were then reoptimized at the higher PBE0+D3/Def2-TZVPP[41] level of theory using the same program. The same level of theory was also employed to compute harmonic frequencies, which were scaled by 0.965. The relative energies determined at the PBE0+D3/Def2-TZVPP level of theory for Met^-, its HOCl adducts, $MetO^-{\cdot}HCl$, $MetO^-$/MetO, $Met^-{\cdot}H_2O$, and $MetO^-{\cdot}H_2O$/$MetO{\cdot}H_2O$ can be found in **Tables S2–S9** respectively. Following this conformational search, the potential energy surface (PES) for the oxidation of Met^- by HOCl was computed by intrinsic reaction coordinate (IRC) calculations performed at the PBE0+D3/Def2-TZVPP level of theory. A detailed description of the computational methods can be found in **Section S2** of the **Supporting Information**.

3. RESULTS AND DISCUSSION

3.1. Interaction of Bare Met^- with HOCl

The mass spectrum obtained upon colliding unsolvated Met^- (**Figure 2a**) with HOCl is displayed in **Figure 2b**. The only significant anionic product is found to be Cl^-. Although this is consistent with the reaction partner incorporating the OH moiety to form a neutral, it is not possible to determine the chemical nature of this species since our characterization method involves cryogenic vibrational spectroscopy of ions. Reaction of bare Met^- with HOCl is expected to yield two very exothermic products (*vide infra*, **Figure 5**):

$$Met^- + HOCl \rightarrow MetO^- + HCl + 152\ \text{kJ mol}^{-1} \quad (2a)$$

$$\rightarrow MetOH + Cl^- + 140\ \text{kJ mol}^{-1} \quad (2b)$$

As such, we might have expected both channels to be populated with a branching ratio associated with fragmentation of an H-bonded $MetO{\cdots}H{\cdots}Cl^-$ complex as opposed to the observed exclusive formation of Cl^-. The important observation for this study is that *$MetO^-$ is not formed by collisions between the bare anion and HOCl*. The origin of the Cl^- product is ambiguous at this point, since it could also potentially result from residual Cl_2 that is inherently generated in the HOCl sample preparation.[8, 33] Another complication arises because the reactant mass distribution (**Figure 2a**) includes an additional species at *m/z* = 47 that also cannot be completely ruled out as a precursor to Cl^-. This species is generated directly from the ESI ion source, most likely from collisions in the high-pressure region. It can be formed, for example, by controlled collision-induced dissociation of the Met^- parent. The exact mass determined by the high-resolution MS-MS spectrum presented in **Figure S1** is consistent with cleavage of CH_3S^- (see **Section S1** for additional details).

3.2. Reactive Uptake of HOCl by $Met^-{\cdot}(H_2O)_n$ Clusters

The mass spectrum obtained by colliding a distribution of Met^- water complexes, $Met^-{\cdot}(H_2O)_{n=0\text{-}8}$ (**Figure 2c**), with HOCl in the collision cell is presented in **Figure 2d**. In addition to the Cl^- ion observed

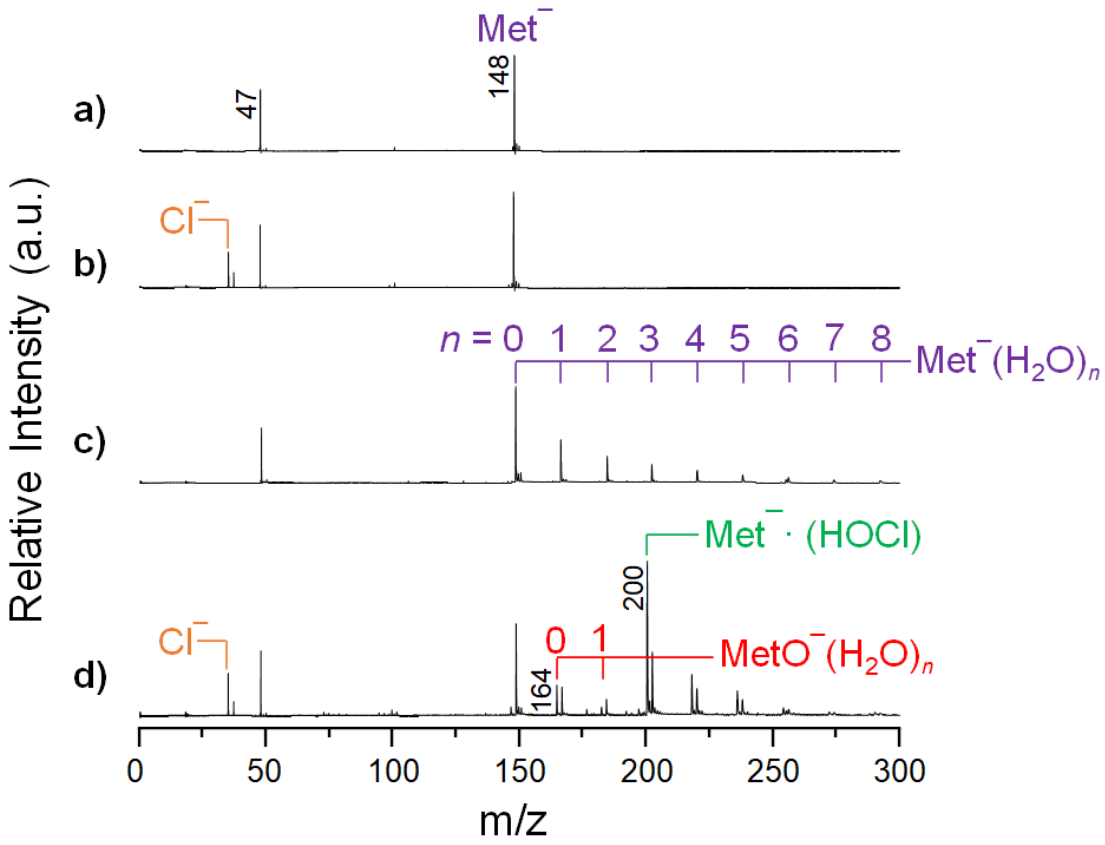

Figure 2. Mass spectra of the reaction between $Met^-\cdot(H_2O)_n$ and HOCl, where n is the number of H_2O solvent molecules: (a) Bare (solventless) Met^- anion (m/z = 148), (b) after collisions between the bare Met^- in (a) and gaseous HOCl in the first quadrupole guide, (c) $Met^-\cdot(H_2O)_n$ cluster series (purple) generated in the ESI ion source, (d) product ion distribution generated by reaction between $Met^-\cdot(H_2O)_n$ in (c) and gaseous HOCl, with product series built on m/z = 164 and the dominant m/z = 200 product labeled in red and green, respectively. The species observed at m/z = 47 in (a)-(d) is a fragment of the parent Met^- anion, as revealed by the mass-selected collision-induced dissociation spectrum in **Figure S1**.

for the bare anion, these collisions yield a water-cluster series (labeled red in **Figure 2d**) built on an anion with m/z = 164, which is displaced 16 Da above the $Met^-\cdot(H_2O)_n$ reactant clusters. This suggests that capture of the expected $MetO^-$ oxidation product (m/z = 164) requires at least one water molecule to be present in the collision complex. A likely scenario is that one or more of the water molecules acts to stabilize the "exit-channel" of the reaction as we discuss further in Section 3.3.

In order to identify the structure of the observed m/z = 164 product, we obtained its vibrational spectrum using the H_2-tagging method.[29-31] The vibrational spectra of the H_2-tagged Met^- reactant anion and its anticipated $MetO^-$ oxidation product are presented in **Figures 3a** and **3b**, respectively, where the latter was generated by ESI of a 4 mM solution of a commercial $MetO^-$ sample (Sigma-Aldrich ≥98%) in 1:9 H_2O/CH_3CN. The only significant difference between the Met^- and $MetO^-$ spectra that is predicted at the PBE0+D3/Def2-TZVPP level of theory (**Figure S2**) is the emergence of the S=O stretching motion ($\nu_{S=O}$) around ~1100 cm^{-1}. Indeed, the experimental spectra of Met^- and $MetO^-$ are strikingly similar, with the exception of the feature at 1070 cm^{-1} (orange) that occurs in the $MetO^-$ spectrum, which we therefore assign to the $\nu_{S=O}$ vibrational fundamental arising from the S=O stretch. The m/z = 164 species generated by reaction of $Met^-\cdot(H_2O)_n$ clusters with HOCl is presented in **Figure 3c**, and indeed contains features

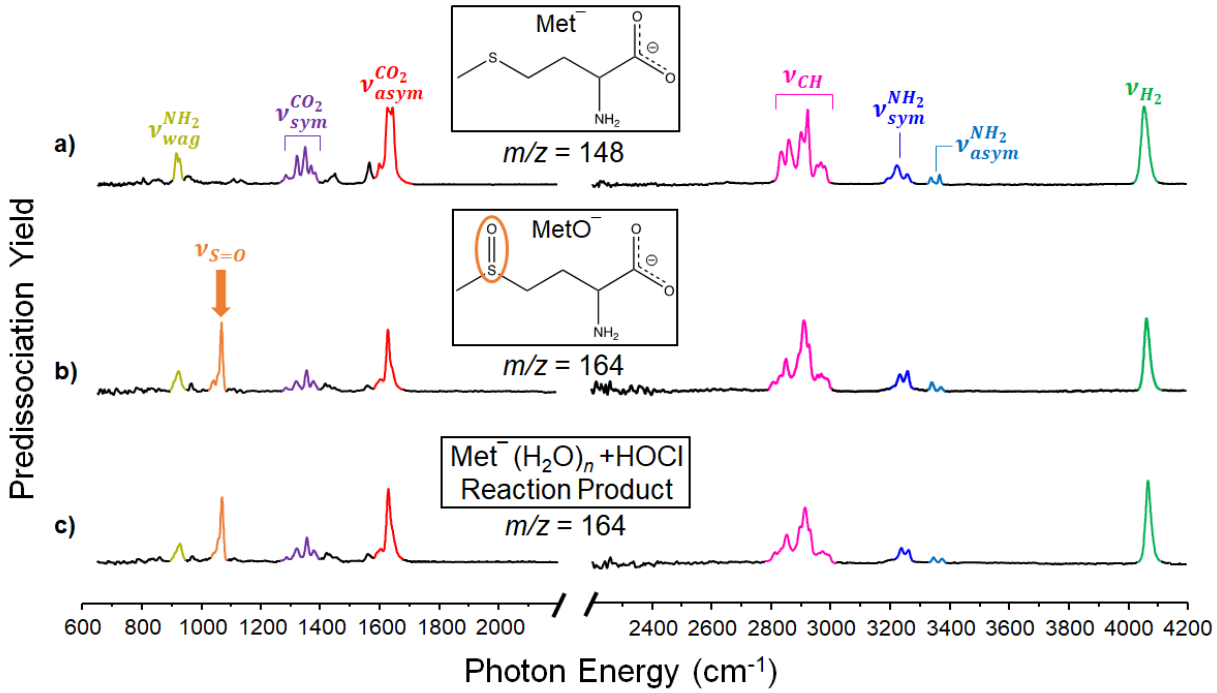

Figure 3. Vibrational predissociation spectra of the H_2-tagged (a) Met^-, (b) commercial $MetO^-$, and (c) the *m/z* = 164 product formed by collisions of $Met^-\cdot(H_2O)_n$ with gaseous HOCl. Two-dimensional illustrations of each species are provided in the insets, while the S=O stretching (labeled $\nu_{S=O}$) is indicated by the orange arrow in (b). A full summary of band labels and assignments, calculated vibrational frequencies, and three-dimensional minimum energy structures can be found in **Table S1** and **Figure S2**.

essentially identical to those displayed by $MetO^-$ (**Figure 3b**), thus confirming that HOCl oxidation of Met^- occurs by formation of the S=O bond. We note here that the oxidation of L-methionine [= (*S*)-methionine] to $MetO^-$ by HOCl creates a new stereocenter at the sulfur atom such that two possible epimers (*R,S*)- and (*S,S*)-$MetO^-$ may be observed. The commercial $MetO^-$ sample is sold as ~1:1 mixture of these two forms, and comparison of the commercial and HOCl product spectra in **Figures 3b** and **3c** are indistinguishable. However, the calculated spectral differences between the two epimers are sufficiently small (**Figure S8**), that we cannot definitely establish the roles of each epimer in the reactive chemistry.

3.3. Nature of the Products with Stoichiometry $Met^-\cdot(HOCl)(H_2O)_n$

In addition to the $MetO^-\cdot(H_2O)_n$ series, a second product ion located 52 Da above Met^- (*m/z* = 200, labeled green in **Figure 2d**) with a stoichiometry consistent with the formation of a complex between Met^- and HOCl actually dominates the mass spectrum. The isotope distribution of this 200 Da product is consistent with this assignment, but the peaks appearing displaced by ~18 Da above it appear with a different isotope pattern. For example, the species located near 218 Da has a 218/220/222 ratio of about 9:6:1, which is consistent with formation of $Met^-\cdot(Cl_2)(H_2O)_n$, expected from "ligand exchange" of residual Cl_2 with a water molecule on the reactant cluster ion. Additional mass degeneracies with $Met^-\cdot(H_2O)_n$ and $Met^-\cdot(HOCl)(H_2O)_n$ complicate the classification of this cluster distribution, and we therefore focus here on the *m/z* = 200 major product because it is unambiguously assigned to a species with composition $Met^-\cdot(HOCl)$.

The H_2-tagged vibrational spectrum of the *m/z* = 200 ion is shown in **Figure 4b** along with that of the previously discussed *m/z* = 164 $MetO^-$ oxidation product (**Figure 4a**) for comparison. It is immediately clear that the feature at 1070 cm^{-1} previously assigned to $\nu_{S=O}$ in $MetO^-$ is also observed for this species. The presence of the $\nu_{S=O}$ band and the fact that it remains essentially unperturbed indicates that the spectrum in **Figure 4b** represents an exit-channel complex in which the S=O bond has already formed. As such, it is anticipated that this species features attachment of the HCl acid molecule to the anionic charge center on the $MetO^-$ product. The large (108 cm^{-1}) blue-shift of the CO_2 asymmetric stretch ($\nu_{asym}^{CO_2}$) relative to that found in the $MetO^-$ anion (labeled Δ_{as}^{CO} in **Figure 4**) is indeed consistent with an arrangement in which the HCl leaving group binds to one of the C–O oscillators in the $-CO_2^-$ group. This blue-shift is predicted (78 cm^{-1}) at the PBE0+D3/Def2-TZVPP level of theory for the minimum energy structure recovered along the reaction coordinate (see **Section S2** and **Figure S2**), where the proton is shared asymmetrically between the C–O group and Cl^-. The vibrational transition associated with parallel stretching motion of the shared-proton is predicted to occur at 2727 cm^{-1} (black arrow labeled ν_{sp}^{calc} in **Figure 4b**) with a large intensity enhancement. This falls roughly in the middle of a strong series of bands (aqua in **Figure 4b**) that are not present in the $MetO^-$ spectrum. This envelope is dramatically red-shifted from the fundamental in isolated HCl (by 183 cm^{-1}),[42] and conforms to the behavior of systems with a strongly shared "excess proton" between anionic bases (in this case, $-CO_2^-$ and Cl^-).[43] In such cases, it is typical that the oscillator strength predicted at the harmonic level is distributed among many nearby levels through strong anharmonic coupling to vibrational modes associated with the two partners.[44] When this

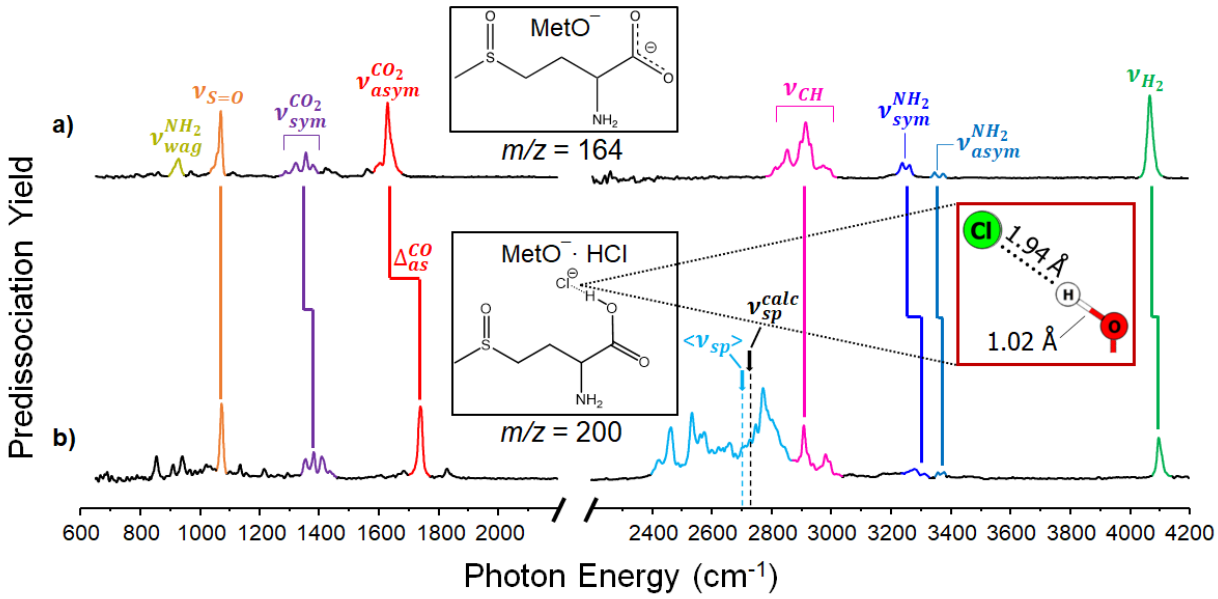

Figure 4. H_2-tagged vibrational predissociation spectra of (a) $MetO^-$ and (b) the $MetO^-$·HCl exit-channel complex, both formed by collisions of Met^-·$(H_2O)_n$ with gaseous HOCl. Two-dimensional illustrations of each species are provided in the insets. The S=O stretching (labeled $\nu_{S=O}$) and CO_2 asymmetric stretching (labeled $\nu_{asym}^{CO_2}$) motions are colored in orange and red, respectively. The calculated geometry (PBE0+D3/Def2-TZVPP level of theory) of the shared-proton motif in the (*S*-*S*)-configuration of $MetO^-$·HCl is also displayed in (b). The calculated (PBE0+D3/Def2-TZVPP, scaled by 0.965) and observed centroid of the transitions (aqua) associated with the bridging proton in this motif are indicated by the black arrows in (b) labeled ν_{sp}^{calc} and $<\nu_{sp}>$, respectively (see text). The blue-shift of $\nu_{asym}^{CO_2}$ upon complexation with HCl is denoted Δ_{as}^{CO}. A full summary of band labels and assignments, calculated vibrational frequencies, and three-dimensional minimum energy structures can be found in **Table S1** and **Figure S2**.

occurs, a useful parameter to quantify the spectral behavior of shared-proton motion is the centroid of the bands associated with it. In this case, the centroid of the aqua bands occurs at 2702 cm^{-1} (arrow labeled $<\nu_{sp}>$ in **Figure 4b**), very close to the calculated harmonic value (ν_{sp}^{calc} = 2727 cm^{-1}) for the parallel motion of the bridging proton. Although this supports the structural assignment of the HOCl uptake species as the proton-bound, exit-channel complex ($MetO^-\cdot HCl$), explicit calculation of these effects is computationally demanding. To critically assess this hypothesis, we therefore turned to an empirical approach in which we acquired the H_2-tagged spectrum of the $CH_3COO^-\cdot HCl$ binary complex. This species was formed by collisions of $Cl^-\cdot(H_2O)_n$ clusters with acetic acid vapor in the first quadrupole guide (see **Figure S3**) in order to obtain the vibrational signature of the isolated $COO\cdots H\cdots Cl^-$ motif. As expected, its shared proton band (ν_{sp}) appears in a similar region of the spectrum (**Figure S4**) with a multiplet structure centered at 2763 cm^{-1}. The agreement with our observations of the locations of the diffuse bands in the spectrum of the *m/z* = 200 ion thus supports the conclusion that this species corresponds to a structure in which the HCl molecule is strongly bound to the carboxylate group of the $MetO^-$ product ion.

3.4. Comments on Mechanism of Cluster-mediated Product Formation

To help clarify the observed chemical pathways (Cl^- formed by reaction with bare Met^-, $MetO^-$ formed only in the presence of $Met^-\cdot(H_2O)_n$), we calculated the stationary points along the reactive potential energy surface (PES) with the results displayed in **Figure 5**. Additional computational details can be found in **Section S2** of the **Supporting Information**. The reaction is calculated to be initiated by the preferential binding of HOCl to the $-CO_2^-$ headgroup to form a pre-reaction complex (**Int1**). The oxygen atom of HOCl

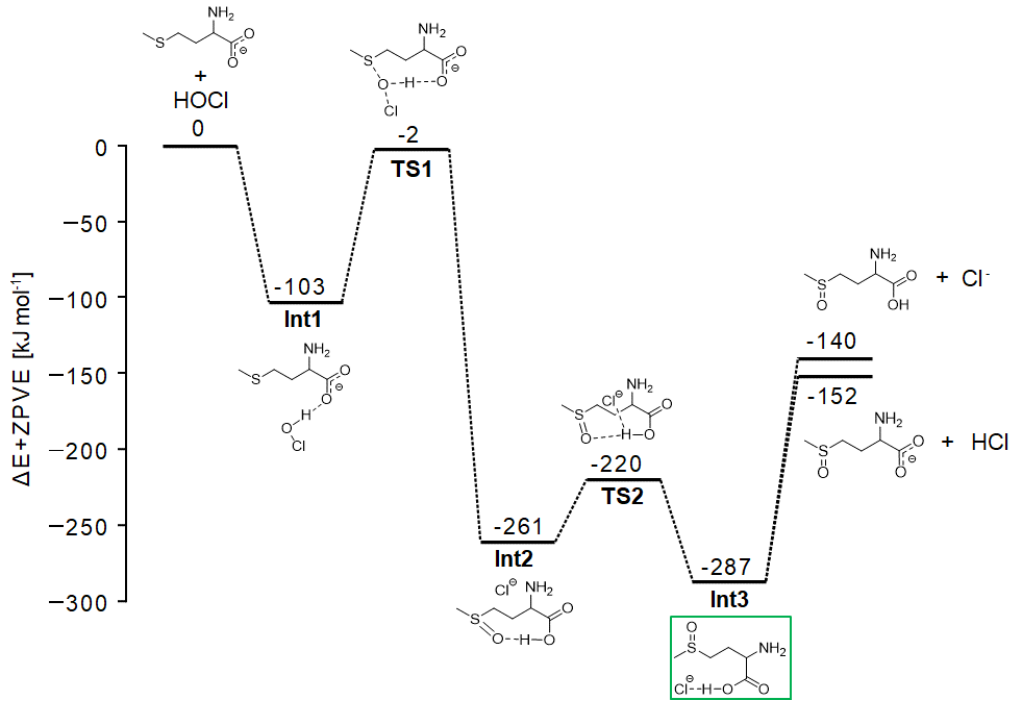

Figure 5. Stationary point calculations of the potential energy surface (PES) for the oxidation of Met^- by HOCl to form (*S*-*S*)-$MetO^-$/MetO, performed at the PBE0+D3/Def2-TZVPP level of theory. The observed exit-channel complex containing a $COOH\cdots Cl^-$ motif is indicated by the green rectangle. The complementary PES yielding the (*R*,*S*)-configuration of $MetO^-$ is reported in **Figure S5**. Further computational details can be found in **Section S2** of the **Supporting Information**.

then directly attacks the sulfur atom to form a cyclic structure with an S···O···H motif (**TS1**) reminiscent of the oxysulfonium species proposed by Ruff *et al*[27] (**Scheme 1b**), but with the proton shared by the neighboring carboxylate. A key feature of the PES is the predicted release of 259 kJ mol^{-1} upon formation of the S=O bond following **TS1**. The resulting species (**Int2**) is essentially an ion-molecule complex involving Cl^- attachment to an organic scaffold with N-H…Cl^- and multiple C-H…Cl^- contacts driven by dispersion rather than specific hydrogen bonding. As such, it is likely that this nascent species has sufficient energy to dissociate, leading to the observed exclusive formation of Cl^-, since formation of HCl would require substantial rearrangement of the organic group. This also provides a natural mechanism for the cluster-mediated observation of $MetO^-$ as well as the exit-channel complex, $MetO^-$·HCl. The situation is reminiscent of cluster-mediated "cage recombination" experiments reported in the 1990s, in which the substantial recoil energy imparted to nascent products from photodissociation (e.g., $I_2^- + h\nu \rightarrow I + I^-$) could be suppressed by energy transfer to solvent molecules in the anionic clusters.[45-46] In the limit that the fragmentation branching ratio is controlled by cluster energetics, the energy released upon recombination of Cl^- with MetO to form **Int3** in **Figure 5** is dissipated by sequential evaporation of the water molecules:

$$\begin{aligned} \mathrm{Met^-}\cdot(\mathrm{H_2O})_n + \mathrm{HOCl} \rightarrow [\mathrm{Cl^-}\cdots\mathrm{MetO}]^*\cdot(\mathrm{H_2O})_n \rightarrow\rightarrow [\mathrm{MetO^-}\cdots\mathrm{HCl}]\cdot(\mathrm{H_2O})_{n-m} + m\mathrm{H_2O} \\ \rightarrow \mathrm{MetO^-} + \mathrm{HCl} + n\mathrm{H_2O} \end{aligned} \quad (3)$$

Since the binding energy of $MetO^-$ to HCl is calculated to be roughly twice as strong as that to H_2O (see **Figure S6** for the n = 1 H_2O PES), we expect selective H_2O loss until all water ligands are gone, at which point HCl is finally ejected from the strongly bound core ion complex. In this scenario, formation of **Int3** releases 287 kJ mol^{-1}, and given the calculated binding energy of $MetO^-$ to water (65 kJ mol^{-1}) the parent cluster would have to contain at least 4 or 5 molecules to leave the exit-channel complex intact. The fact that the $MetO^-$·HCl exit-channel dominates the product distribution is consistent with this mechanism. These mechanistic considerations emphasize the importance of carrying out future experiments to establish the cluster size-dependence of the uptake reactions, which will require reconfiguration of the photofragmentation mass spectrometer used for this work. In addition, systemically varying the solvent molecules in the Met^-·(solvent)$_n$ reactant clusters would provide a useful test on the solvent evaporation model (as opposed to chemical participation by H_2O, perhaps through proton-transfer). Preliminary work interrogating the collisions of Met^-·$(CH_3OH)_n$ clusters with HOCl (**Figure S7**) similarly yields product masses corresponding to both the $MetO^-$·HCl exit-channel complex as well as the bare $MetO^-$ species. This underscores the spectator role of the solvent, which appears to act as a third body to accommodate the excess energy released in the reaction by means of evaporation.

4. SUMMARY

We have reported the gas-phase HOCl oxidation of the conjugate base of methionine complexed with water molecules. At least one solvent molecule is required to generate product anions based in the methionine scaffold. The products arising from HOCl uptake were characterized by analysis of their vibrational spectra obtained by infrared photodissociation of weakly-bound H_2 tags. These spectra confirm formation of the expected sulfoxide bond to yield the $MetO^-$ anion, while the species corresponding to addition of HOCl is revealed to be an exit-channel, ion-molecule complex in which the HCl leaving group remains bound to the -CO_2^- site of $MetO^-$. Stationary point calculations of the potential energy surface support a mechanism in which HOCl is first captured by the -CO_2^- group before forming a cyclic transition state with an S···O···H motif.

ASSOCIATED CONTENT

The **Supporting Information** is available free of charge on the ACS Publications website.

Additional experimental and computational details, vibrational band labels and assignments, relative energies of lowest-energy conformations sampled by CREST, and supplementary figures.

xyz-coordinates and absolute energies of all reoptimized structures (coordinates.xyz).

AUTHOR INFORMATION

Corresponding Authors

Mark A. Johnson - *Sterling Chemistry Laboratory, Department of Chemistry, Yale University, New Haven, CT 06520, United States;*
orcid.org/0000-0002-1492-6993
Email: mark.johnson@yale.edu

Authors

Santino J. Stropoli - *Sterling Chemistry Laboratory, Department of Chemistry, Yale University, New Haven, CT 06520, United States;*
orcid.org/0000-0003-4203-5060

Kim Greis - *Sterling Chemistry Laboratory, Department of Chemistry, Yale University, New Haven, CT 06520, United States; Institut für Chemie und Biochemie, Freie Universität Berlin, Altensteinstraße 23A, 14195 Berlin, Germany; Fritz-Haber-Institut der Max-Planck-Gesellschaft, Faradayweg 4–6, 14195 Berlin, Germany*
orcid.org/0000-0002-9107-2282

Tim Schleif - *Sterling Chemistry Laboratory, Department of Chemistry, Yale University, New Haven, CT 06520, United States;*
orcid.org/0000-0003-0154-9540

Notes

The authors declare no competing financial interest.

Data used to generate figures is publicly available in a dataset hosted by the UCSD Library Digital Collections at: https://doi.org/10.6075/J0DF6RDD

ACKNOWLEDGEMENTS

This work was supported by NSF through the NSF Center for Aerosol Impacts on Chemistry of the Environment (CAICE), CHE-1801971. Any opinions, findings, and conclusions or recommendations expressed in this material are those of the author(s) and do not necessarily reflect the views of the National Science Foundation (NSF). K.G. thanks the Fonds National de la Recherche, Luxembourg, for funding the project GlycoCat (13549747) and the Fulbright Program for funding his research stay at Yale University. T.S. was supported by a Walter-Benjamin Scholarship by the Deutsche Forschungsgemeinschaft (Projektnummer 459401225). This research made use of the Chemical and Biophysical Instrumentation Center at Yale University (RRID:SCR_021738).

REFERENCES

(1) Simpson, W. R.; Brown, S. S.; Saiz-Lopez, A.; Thornton, J. A.; von Glasow, R. Tropospheric Halogen Chemistry: Sources, Cycling, and Impacts. *Chem. Rev.* **2015,** *115* (10), 4035-4062.

(2) Faxon, C. B.; Allen, D. T. Chlorine Chemistry in Urban Atmospheres: A Review. *Environ. Chem.* **2013,** *10* (3), 221-233.

(3) Burkholder, J. B.; Cox, R. A.; Ravishankara, A. R. Atmospheric Degradation of Ozone Depleting Substances, Their Substitutes, and Related Species. *Chem. Rev. (Washington, DC, U. S.)* **2015,** *115* (10), 3704-3759.

(4) Davies, M. J.; Hawkins, C. L.; Pattison, D. I.; Rees, M. D. Mammalian heme peroxidases: From molecular mechanisms to health implications. *Antioxid. Redox Sign.* **2008,** *10* (7), 1199-1234.

(5) Klebanoff, S. J.; Kettle, A. J.; Rosen, H.; Winterbourn, C. C.; Nauseef, W. M. Myeloperoxidase: a front-line defender against phagocytosed microorganisms. *J. Leukoc. Biol.* **2013,** *93* (2), 185-198.

(6) Vogt, R.; Crutzen, P. J.; Sander, R. A mechanism for halogen release from sea-salt aerosol in the remote marine boundary layer. *Nature* **1996,** *383* (6598), 327-330.

(7) Pechtl, S.; von Glasow, R. Reactive chlorine in the marine boundary layer in the outflow of polluted continental air: A model study. *Geophys. Res. Lett.* **2007,** *34* (11).

(8) Lawler, M. J.; Sander, R.; Carpenter, L. J.; Lee, J. D.; von Glasow, R.; Sommariva, R.; Saltzman, E. S. HOCl and Cl_2 observations in marine air. *Atmos. Chem. Phys.* **2011,** *11* (15), 7617-7628.

(9) Pratte, P.; Rossi, M. J. The heterogeneous kinetics of HOBr and HOCl on acidified sea salt and model aerosol at 40-90% relative humidity and ambient temperature. *Phys. Chem. Chem. Phys.* **2006,** *8* (34), 3988-4001.

(10) Bratsch, S. G. Standard Electrode-Potentials and Temperature Coefficients in Water at 298.15-K. *J. Phys. Chem. Ref. Data* **1989,** *18* (1), 1-21.

(11) O'Dowd, C. D.; Facchini, M. C.; Cavalli, F.; Ceburnis, D.; Mircea, M.; Decesari, S.; Fuzzi, S.; Yoon, Y. J.; Putaud, J. P. Biogenically driven organic contribution to marine aerosol. *Nature* **2004,** *431* (7009), 676-80.

(12) Bertram, T. H.; Cochran, R. E.; Grassian, V. H.; Stone, E. A. Sea spray aerosol chemical composition: elemental and molecular mimics for laboratory studies of heterogeneous and multiphase reactions. *Chem Soc Rev* **2018,** *47* (7), 2374-2400.

(13) Hawkins, C. L.; Pattison, D. I.; Davies, M. J. Hypochlorite-induced oxidation of amino acids, peptides and proteins. *Amino Acids* **2003,** *25* (3-4), 259-274.

(14) Triesch, N.; van Pinxteren, M.; Salter, M.; Stolle, C.; Pereira, R.; Zieger, P.; Herrmann, H. Sea Spray Aerosol Chamber Study on Selective Transfer and Enrichment of Free and Combined Amino Acids. *ACS Earth Space Chem.* **2021,** *5* (6), 1564-1574.

(15) Storkey, C.; Davies, M. J.; Pattison, D. I. Reevaluation of the rate constants for the reaction of hypochlorous acid (HOCl) with cysteine, methionine, and peptide derivatives using a new competition kinetic approach. *Free Radic. Biol. Med.* **2014,** *73*, 60-66.

(16) Angle, K. J.; Nowak, C. M.; Davasam, A.; Dommer, A. C.; Wauer, N. A.; Amaro, R. E.; Grassian, V. H. Amino Acids Are Driven to the Interface by Salts and Acidic Environments *J Phys Chem Lett* **2022,** *13* (12), 2824-2829.

(17) Herboth, R.; Gopakumar, G.; Caleman, C.; Wohlert, M. Charge State Dependence of Amino Acid Propensity at Water Surface: Mechanisms Elucidated by Molecular Dynamics Simulations. *J. Phys. Chem. A* **2021,** *125* (22), 4705-4714.

(18) Campbell, N. R.; Ryder, O. S.; Bertram, T. H. In *Reactive uptake of HOCl to laboratory generated sea salt particles and nascent sea-spray aerosol*, American Geophysical Union Fall Meeting Abstracts, 2013.

(19) Harrison, J. E.; Schultz, J. Studies on the chlorinating activity of myeloperoxidase. *J Biol Chem* **1976,** *251* (5), 1371-4.

(20) Thomas, E. L. Myeloperoxidase, hydrogen peroxide, chloride antimicrobial system: nitrogen-chlorine derivatives of bacterial components in bactericidal action against Escherichia coli. *Infect Immun* **1979,** *23* (2), 522-31.
(21) Albrich, J. M.; McCarthy, C. A.; Hurst, J. K. Biological reactivity of hypochlorous acid: implications for microbicidal mechanisms of leukocyte myeloperoxidase. *Proc Natl Acad Sci U S A* **1981,** *78* (1), 210-4.
(22) Pattison, D. I.; Davies, M. J. Absolute rate constants for the reaction of hypochlorous acid with protein side chains and peptide bonds. *Chem Res Toxicol* **2001,** *14* (10), 1453-1464.
(23) Armesto, X. L.; Canle, M.; Fernandez, M. I.; Garcia, M. V.; Santaballa, J. A. First steps in the oxidation of sulfur-containing amino acids by hypohalogenation: Very fast generation of intermediate sulfenyl halides and halosulfonium cations. *Tetrahedron* **2000,** *56* (8), 1103-1109.
(24) Peskin, A. V.; Winterbourn, C. C. Kinetics of the reactions of hypochlorous acid and amino acid chloramines with thiols, methionine, and ascorbate. *Free Radical Biology and Medicine* **2001,** *30* (5), 572-579.
(25) Wilson, G. E. Structure and Reactivity of Halosulfonium Salts. *Tetrahedron* **1982,** *38* (17), 2597-2625.
(26) Beal, J. Measuring Rate Constants for the Reaction of Hypochlorous Acid and Biologically Relevant Molecules University of Oklahoma, 2012.
(27) Ruff, F.; Jalsovszky, I.; Szabo, D.; Rabai, J.; Farkas, O.; Kucsman, A. Mechanism for the reactions of sulfides and sulfoxides with hypochlorites: racemization and oxygen exchange of oxysulfonium salts and sulfoxides. *J Phys Org Chem* **2012,** *25* (12), 1086-1096.
(28) Ruff, F.; Szabo, D.; Rabai, J.; Jalsovszky, I.; Farkas, O. Mechanism for the reactions of sulfides with hypochlorous acid and N-chlorosulfon-amides: Formation of solvated chlorosulfonium cation and lambda(4)-sulfane intermediates. *J Phys Org Chem* **2019,** *32* (11), e4005.
(29) Wolk, A. B.; Leavitt, C. M.; Garand, E.; Johnson, M. A. Cryogenic Ion Chemistry and Spectroscopy. *Acc. Chem. Res.* **2014,** *47* (1), 202-210.
(30) Yang, N.; Duong, C. H.; Kelleher, P. J.; Johnson, M. A.; McCoy, A. B. Isolation of Site-Specific Anharmonicities of Individual Water Molecules in the $I^-\cdot(H_2O)_2$ Complex Using Tag-Free, Isotopomer Selective IR-IR Double Resonance. *Chem. Phys. Lett.* **2017,** *690*, 159-171.
(31) Menges, F. S.; Perez, E. H.; Edington, S. C.; Duong, C. H.; Yang, N.; Johnson, M. A. Integration of High-Resolution Mass Spectrometry with Cryogenic Ion Vibrational Spectroscopy. *J. Am. Soc. Mass Spectrom.* **2019,** *30* (9), 1551-1557.
(32) Stropoli, S. J.; Khuu, T.; Messinger, J. P.; Karimova, N. V.; Boyer, M. A.; Zakai, I.; Mitra, S.; Lachowicz, A. L.; Yang, N.; Edington, S. C., et al. Preparation and Characterization of the Halogen-Bonding Motif in the Isolated $Cl^-\cdot$IOH Complex with Cryogenic Ion Vibrational Spectroscopy. *J Phys Chem Lett* **2022,** *13* (12), 2750-2756.
(33) Stropoli, S. J.; Khuu, T.; Boyer, M. A.; Karimova, N. V.; Gavin-Hanner, C. F.; Mitra, S.; Lachowicz, A. L.; Yang, N.; Gerber, R. B.; McCoy, A. B., et al. Electronic and mechanical anharmonicities in the vibrational spectra of the H-bonded, cryogenically cooled $X^- \cdot$ HOCl (X=Cl, Br, I) complexes: Characterization of the strong anionic H-bond to an acidic OH group. *J. Chem Phys.* **2022,** *156* (17), 174303.
(34) Marsh, B. M.; Voss, J. M.; Garand, E. A Dual Cryogenic Ion Trap Spectrometer for the Formation and Characterization of Solvated Ionic Clusters. *J. Chem. Phys.* **2015,** *143* (20), 204201.
(35) Pracht, P.; Bohle, F.; Grimme, S. Automated exploration of the low-energy chemical space with fast quantum chemical methods. *Phys. Chem. Chem. Phys.* **2020,** *22* (14), 7169-7192.
(36) Bannwarth, C.; Ehlert, S.; Grimme, S. GFN2-xTB-An Accurate and Broadly Parametrized Self-Consistent Tight-Binding Quantum Chemical Method with Multipole Electrostatics and Density-Dependent Dispersion Contributions. *J. Chem. Theory Comput.* **2019,** *15* (3), 1652-1671.

(37) Frisch, M. J.; Trucks, G. W.; Schlegel, H. B.; Scuseria, G. E.; Robb, M. A.; Cheeseman, J. R.; Scalmani, G.; Barone, V.; Petersson, G. A.; Nakatsuji, H., et al. *Gaussian 16 Rev. A.03*, Wallingford, CT, **2016**.
(38) Adamo, C.; Barone, V. Toward reliable density functional methods without adjustable parameters: The PBE0 model. *J. Chem. Phys.* **1999,** *110* (13), 6158-6170.
(39) Grimme, S.; Antony, J.; Ehrlich, S.; Krieg, H. A Consistent and Accurate Ab Initio Parametrization of Density Functional Dispersion Correction (DFT-D) for the 94 Elements H-Pu. *J. Chem. Phys.* **2010,** *132* (15), 154104.
(40) Hehre, W. J.; Ditchfield, R.; Pople, J. A. Self—Consistent Molecular Orbital Methods. XII. Further Extensions of Gaussian—Type Basis Sets for Use in Molecular Orbital Studies of Organic Molecules. *J. Chem. Phys.* **1972,** *56* (5), 2257-2261.
(41) Weigend, F.; Ahlrichs, R. Balanced Basis Sets of Split Valence, Triple Zeta Valence and Quadruple Zeta Valence Quality for H to Rn: Design and Assessment of Accuracy. *Phys. Chem. Chem. Phys.* **2005,** *7* (18), 3297-3305.
(42) Coblentz Society, Inc. Evaluated Infrared Reference Spectra. In *NIST Chemistry WebBook, NIST Standard Reference Database Number 69*, Linstrom, P. J.; Mallard, W. G., Eds. National Institute of Standards and Technology: Gaithersburg MD, 20899, 2022.
(43) Roscioli, J. R.; McCunn, L. R.; Johnson, M. A. Quantum Structure of the Intermolecular Proton Bond. *Science* **2007,** *316*, 249-254.
(44) Leavitt, C. M.; DeBlase, A. F.; van Stipdonk, M.; McCoy, A. B.; Johnson, M. A. Hiding in Plain Sight: Unmasking the Diffuse Spectral Signatures of the Protonated N-Terminus in Simple Peptides. *J Phys Chem Lett* **2013,** *4*, 3450-3457.
(45) Papanikolas, J. M.; Gord, J. R., Jr.; Levinger, N. E.; Ray, D.; Vorsa, V.; Lineberger, W. C. Photodissociation and geminate recombination dynamics of I2- in mass-selected I2-(CO2)n cluster ions. *J. Phys. Chem.* **1991,** *95*, 8028-8040.
(46) Lavrich, D. J.; Buntine, M. A.; Johnson, M. A. Excess energy-dependent photodissociation probabilities of O_2^- in water cluster: $O_2^{-}\cdot(H_2O)_n$, $1<n<33$. *J. Phys. Chem.* **1995,** *99*, 8453.